Int. J. Solids Structures, 1976, Vol. 12, pp. 377-389. Pergamon Press. Printed in Great Britain

THE EVOLUTION OF CAUSTICS FROM HOLES TO CRACKS

P. S. THEOCARIS

Department of Theoretical and Applied Mechanics, The National Technical University, Athens (625), Greece

(*Received* 9 *April* 1975; *revised* 11 *October* 1975)

Abstract—The method of caustics was used for the study of the evolution of stress concentration around a circular hole, which progressively changes in shape and becomes an elliptic hole, tending to an internal crack. The influence of the amount of ellipticity of the holes and their orientation relative to the axis of the applied external loads at infinity on the form of caustics created around the discontinuity was studied, as the elliptic holes tended to become internal cracks. A series of experiments with tension specimens containing small elliptic holes of any ellipticity and orientation was performed. Comparison of experimentally obtained caustics with theory yielded a good agreement of both results. Finally, the use of small elliptic holes drilled all over a biaxial stress field for the determination of the individual principal stresses and the principal directions at the area of the holes was outlined.

INTRODUCTION

The method of caustics, as it has been developed by the author[1], proved to be a simple and potential method for studying singularities in stress fields. The strong thickness and refractive index variation at the close vicinity of an elastic stress singularity deviates the impinging light rays from a light bundle which was either reflected from, or transmitted through the transparent plate when loaded. The thus scattered light rays are gathered along a singular surface. The section of this surface with a plane, placed at some distance from the plate, yields a singular curve, *the caustic*. Thus, the stress singularity is transformed into an optical singularity, which yields all the necessary information for studying the respective stress singularity. The same results may be obtained, if, instead of a singularity, any type of stress concentration along a boundary exists, which varies the thickness of the deformed plate[2].

The method of caustics is unique for studying singularities and load concentrations, where all other conventional optical methods, like photoelasticity and moiré, fail to yield accurate results. This method is applied in this paper to study the progressive transformation of the surface topography of perforated plates, when these perforations are successively modified to elliptic holes of different ellipticity and orientation relatively to the external loads, and finally, they are changed to internal cracks. The results obtained were used to formulate a new stress-optic rosette method which yields directly the individual values of principal stresses and their orientation at the point of perforation of the small ellipse.

AN OUTLINE OF THE METHOD OF REFLECTED CAUSTICS

If a monochromatic and coherent light beam, emitted from a He–Ne laser, impinges normally on the lateral faces of a thin-plate made of a transparent material, it is partially reflected from the front and rear faces of the plate, so that an infinite number of rays emerges from the plate. From all these rays we are interested in those reflected once from the front and rear faces of the plate, since the intensity of these two rays is significant relatively to the others[3]. For the light rays reflected form the rear face of the plate, which were retarded as they crossed twice the thickness d of the specimen, the absolute retardations $\Delta s_{r_{1,2}}$ of the light path are expressed by[3]

$$\Delta s_{r_{1,2}} = 2dc_r[(\sigma_1 + \sigma_2) \pm \xi_r(\sigma_1 - \sigma_2)] \tag{1}$$

where

$$c_r = \frac{1}{2E}\left[(b_1 + b_2) - \nu(b_1 + 3b_2) - 2\nu\left(n - \frac{1}{2}\right)\right] \tag{2}$$

and

$$\xi_r = \frac{(1+\nu)(b_1 - b_2)}{\left[(b_1 + b_2) - \nu(b_1 + 3b_2) - 2\nu\left(n - \frac{1}{2}\right)\right]} \tag{3}$$

and $b_{1,2}$ are optical constants relating the variations due to loading of the refractive indices along the principal directions of the plate to the principal strains according to Maxwell–Neumann stress-optical law[4], n is the refractive index of the unloaded material, E and ν the elastic modulus and Poisson's ratio of the material of the plate and $\sigma_{1,2}$ the principal stresses. Indices 1,2 are referred to the two principal stress-optical directions of the plate respectively.

For the optically isotropic materials, like plexiglas, there is $b_1 = b_2$, so that $\xi_r = 0$ and therefore

$$\Delta s_1 = \Delta s_2 = 2dc_r(\sigma_1 + \sigma_2). \tag{4}$$

The emerging light front $S(x, y, z)$ after reflection from the rear face, is given according to the theory of Eikonal[5] by

$$S(x, y, z) = z - s(x, y) = \text{const.} \tag{5}$$

so that,

$$\text{grad } S(x, y, z) = \mathbf{k} - \frac{\partial s}{\partial x}\mathbf{i} - \frac{\partial s}{\partial y}\mathbf{j} \tag{6}$$

where **i**, **j**, **k** is a system of Cartesian unit vectors connected with the plate with the **k**-axis being normal to the plate. If a reference screen Sc is placed at a distance z_r from the rear surface of the plate and parallel to the plate and **w** (**w** = $P'Q'$) expresses the displacement of point P' on the screen due to the deviation of light, then **w** is given by (Fig. 1)

$$\mathbf{w} = -z_r \text{ grad } S(x, y, z)$$

or

$$\mathbf{w} = -z_r\left(\frac{\partial s}{\partial x}\mathbf{i} + \frac{\partial s}{\partial y}\mathbf{j}\right)$$

Since

$$s(x, y) = s_0 + \Delta s_r(x, y)$$

we have

$$\mathbf{w}_r = -z_r \text{ grad } \Delta s_r(x, y).$$

Introducing relation (4) for the reflected from the rear face of the specimen rays we obtain

$$\mathbf{w}_r = -2z_r c_r d \text{ grad } (\sigma_1 + \sigma_2). \tag{7}$$

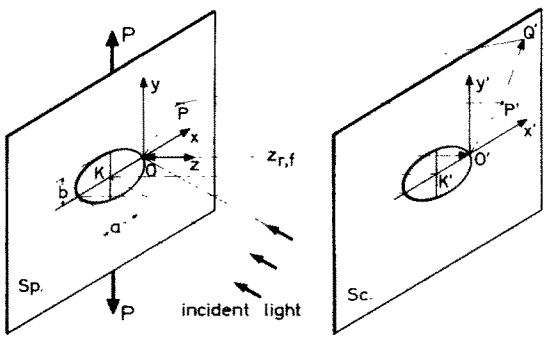

Fig. 1. Geometry of a perforated plate and relative position of specimen and reference screen.

Similarly, it can be shown that the deviation w of the reflected light rays from the front face are given by

$$\mathbf{w}_f = -z_f \frac{\nu d}{E} \operatorname{grad}(\sigma_1 + \sigma_2) \tag{8}$$

where z_f is the distance of the front surface of the plate from the reference screen *Sc*. Relations (7) and (8) may be placed under the same form by putting

$$\mathbf{w}_{r,f} = C \operatorname{grad}(\sigma_1 + \sigma_2) \tag{9}$$

where (i) $C \equiv C_r = -2z_r dc_r$ for reflected from the rear face rays; (ii) $C \equiv C_f = z_f dc_f$ for reflected from the front face rays (with $c_f = -\nu/E$).

Referring the vector $\mathbf{w}_{r,f}$, which expresses the displacement of point P' on the screen due to the deviation of light when the specimen is loaded, to the origin of a fixed coordinate system $O'x'y'$ on screen *Sc* with origin the projection O' of O on *Sc*, we obtain

$$\mathbf{W}_{r,f} = \mathbf{r} + C \operatorname{grad}(\sigma_1 + \sigma_2). \tag{10}$$

According to the complex stress theory developed by Muskhelishvili[6] the sum of principal stresses is expressed by

$$(\sigma_1 + \sigma_2) = 4Re\ \Phi(z) \tag{11}$$

where $\Phi(z)$ is an analytic function of the complex variable z and *Re* expresses the real part of $\Phi(z)$.

Introducing relation (11) into eqn (10) and putting for $\Phi(z)$

$$\Phi(z) = u(x, y) + iv(x, y) \tag{12}$$

we obtain for relation (10) the following expression in complex form

$$W = x' + iy' \tag{13}$$

where

$$x' = x + 4C\frac{\partial u}{\partial x} \quad \text{and} \quad y' = y + 4C\frac{\partial u}{\partial y}.$$

The reflected light rays at the constrained zone surrounding the hole of the perforated strip, due to the lateral contraction of the plate under loading, are deviated by different amounts depending on the slope, as well as on the variation of the refractive index at each point of the constrained zone. These rays are concentrated at an envelope, which thus is strongly illuminated and forms a *caustic*. This limiting envelope represents a singular curve for *W*. The condition of existence of this singular curve is the zeroing of the Jacobian determinant of x', y' with respect to x, y. Thus we have

$$J = \frac{\partial(x', y')}{\partial(x, y)} = 0 \tag{14}$$

and taking into account relations (13) and (14) we obtain

$$4C\left|\frac{d^2\Phi(z)}{dz^2}\right| = -1 \tag{15}$$

Relation (15) expresses the equation of a particular curve on the specimen, called the *initial*

curve, which creates the caustic at the screen. The equation of caustic is expressed by relations (13), which take into account the well known Cauchy–Riemann formulas for an analytic function and it can be written in the form

$$W = z + 4C\overline{\frac{d\Phi(z)}{dz}} \tag{16}$$

where $\overline{d\Phi(z)}/dz$ expresses the conjugate of the first derivative of $\Phi(z)$ with respect to z. Thus, the system of eqns (15) and (16) expresses the relations of the caustic engendered from the initial curve expressed by eqn (15).

THE CAUSTICS IN ELLIPTIC HOLES

Consider now a thin infinite plate containing a stress raiser, such as a central elliptical perforation and subjected to a uniaxial state of stress σ at infinity. A Cartesian frame Oxy is related to the plate with its origin at the center of the performation and the Oy-axis coinciding with the direction of stress σ at infinity. It is assumed that the major axis of the ellipse subtends an angle α with the direction of load.

For the solution of the problem of stress distribution in the plate we use the transformation of the region of the elliptically perforated plate onto the region $|\zeta| > 1$ of an infinite plate with a circular hole [6]. The corresponding transformation is expressed by

$$z = \omega(\zeta) = R\left(\zeta + \frac{m}{\zeta}\right) \quad R > 0 \quad 0 \le m \le 1 \tag{17}$$

where the circle $|\zeta| = 1$ corresponds to the ellipse with center the origin and semi-axes given by

$$a = R(1+m) \quad \text{and} \quad b = R(1-m) \tag{18}$$

where m expresses the ellipticity of the ellipse and R is the radius of the corresponding circle $(R = (a+b)/2)$.

By using the above transformation in combination with the solution of the problem of an infinite plate with a central circular hole given by Muskhelishvili [6] we obtain the following expression for the function $\Phi(z)$

$$\Phi(z) = \frac{\sigma}{4} + \frac{\sigma}{4} \cdot \frac{(e^{2i\alpha} - m)}{m} - \frac{\sigma z}{4m} \frac{(e^{2i\alpha} - m)}{(z^2 - 4mR^2)^{1/2}} \tag{19}$$

This function, differentiated twice with respect to z, yields

$$\begin{aligned} \Phi'(z) &= \sigma R^2 (e^{2i\alpha} - m)(z^2 - 4mR^2)^{-3/2} \\ \overline{\Phi'(z)} &= \sigma R^2 (e^{-2i\alpha} - m)(\bar{z}^2 - 4mR^2)^{-3/2} \\ \Phi''(z) &= -3\sigma R^2 (e^{2i\alpha} - m) z (z^2 - 4mR^2)^{-5/2}. \end{aligned} \tag{20}$$

Introducing these relations into the equations for the caustic and its initial curve, given by relations (15) and (16) we obtain

(i) *For the initial curve*

$$|12\, C\sigma R^{-2}(e^{2i\alpha} - m)(z/R)[(z/R)^2 - 4m]^{-5/2}| = 1 \tag{21}$$

(ii) *For the caustic.* This curve is given by the system of eqn (21) and the following equation

$$(W/R) = (z/R) \pm 4\, C\sigma R^{-2}(e^{-2i\alpha} - m)[(\bar{z}/R)^2 - 4m]^{-3/2}. \tag{22}$$

STUDY OF THE TWO EXTREME CASES: THE CIRCULAR HOLE AND THE INTERNAL CRACK

Equations (21) and (22) for the initial curve and the caustic of a central elliptic hole enable us to study the evolution of the caustic corresponding to a central hole to the caustic corresponding to an internal crack (these are the two limiting cases of the change of ellipticity of the ellipse with $m = 0$ and $m = 1$ respectively).

For the case of a central circular hole corresponding to the one extreme case we obtain from eqns (21) and (22) by putting $m = 0$ the following equations for the initial curve and the caustic

$$|12C\sigma R^2 z^{-4}| = 1 \tag{23}$$

$$W = z \pm 4\, C\sigma R^2 \bar{z}^{-3} \tag{24}$$

respectively.

Equation (23), when solved for $|z|$, yields

$$r = r_0 = |z| = (12\, C\sigma R^2)^{1/4}. \tag{25}$$

Relation (25) indicates that the initial curve is a circle, whose radius r_0 depends on the global constant C, the applied stress σ at infinity and the radius R of the circular hole.

Equation (24), by taking into account relation (25), can be written as ($z = re^{i\theta}$)

$$W = r_0\left(e^{i\theta} \pm \frac{1}{3} e^{3i\theta}\right) \tag{26}$$

or in parametric form as

$$\begin{aligned} X &= r_0\left(\cos\theta \pm \frac{1}{3}\cos 3\theta\right) \\ Y &= r_0\left(\sin\theta \pm \frac{1}{3}\sin 3\theta\right). \end{aligned} \tag{27}$$

Relation (26) suggests that, for the geometric construction of the principal caustic corresponding to an initial curve of radius r_0, a vector of magnitude $(r_0/3)$ from every point of the circumference of the initial curve (with radius r_0) corresponding to angle θ is drawn, under an angle equal to 3θ with the $O'x'$ axis. Figure 2 shows the shape and the relative position of the initial curve, the corresponding caustic and the mode of formation of the caustic from its initial curve.

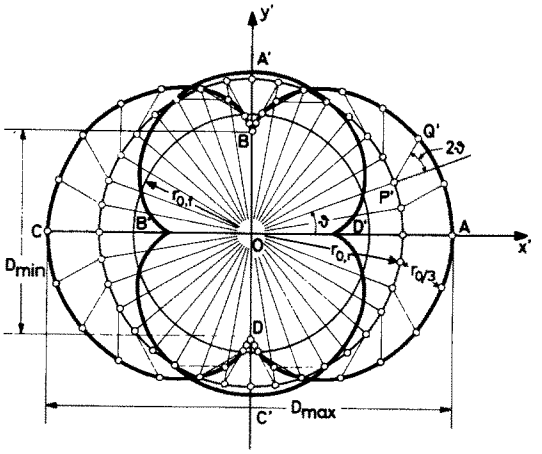

Fig. 2. Geometrical construction of the caustic formed by reflections from the rear face of a specimen with a central circular hole subjected to uniaxial tension at infinity from its initial curve of radius $r_{0,r}$ (circles), and of the caustic formed by reflections from the front face of the specimen with its corresponding initial curve of radius $r_{0,f}$ (broad line), for a plexiglas plate with $2c_r/(\nu/E) = 2{\cdot}68$.

From the above relations it can be concluded that the caustic is a continuous, closed and periodic curve of period 2π and symmetric to both Ox- and Oy-axes.

The equations of the caustic in polar coordinates ρ and ϕ are given by

$$\rho = \frac{r_0}{3}(10 + 6\cos 2\theta)^{1/2}$$
$$\phi = \cot^{-1}\left(\frac{3\cos\theta + \cos 3\theta}{3\sin\theta + \sin 3\theta}\right) \tag{28}$$

From these relations it can be derived that the polar radius ρ presents a maximum for $\theta = 0$ or 2π, where it is valid that

$$\rho_{max} = \frac{4n_0}{3} \quad \text{and} \quad \phi = 0 \quad \text{or} \quad \pi. \tag{29}$$

Furthermore, a minimum for ρ appears for $\theta = \pi/2$ or $3\pi/2$ and

$$\rho_{min} = \frac{2r_0}{3} \quad \text{and} \quad \phi = \frac{\pi}{2} \text{ or } \frac{3\pi}{2}. \tag{30}$$

Thus, it is valid that $\rho_{max} = 2\rho_{min}$. Therefore the maximum diameter of the caustic is twice as large as the corresponding minimum diameter, which is angularly displaced to the former by $\pi/2$.

Figure 3 shows also the relative positions of the two epicycloids formed by reflected light rays for plexiglas, where

$$2c_r = -3{\cdot}24 \times 10^{-5}\ \text{cm}^2/\text{Kp} \quad \text{and} \quad c_f = -\frac{\nu}{E} = -1{\cdot}21 \times 10^{-5}\ \text{cm}^2/\text{Kp}.$$

The ratio between the radii of the initial curves for the caustics formed by reflections from the rear face (Fig. 3 with circles) to that formed by reflections from the front face (Fig. 3 with broad line) of the specimen is $r_r/r_f = 1{\cdot}28$. The same ratio holds for the diameters of the corresponding caustics.

For the other extreme case corresponding to a central crack of length $2a$ in an infinite plate subjected to a uniaxial stress σ at infinity, we obtain from relation (19) by putting $m = 1$ the following form for the singular term of the function $\Phi(z)$

$$\Phi(z) = -\frac{\sigma(e^{2i\alpha} - 1)}{4}\frac{z}{(z^2 - a^2)^{1/2}}.$$

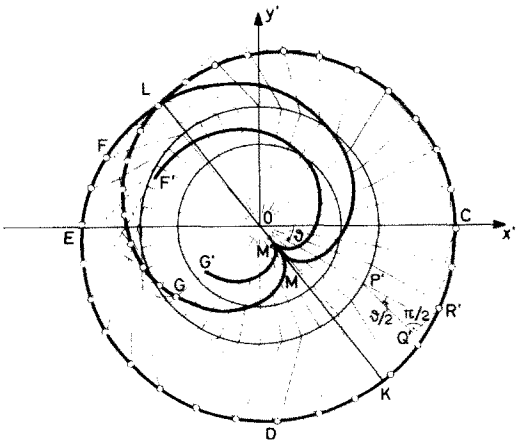

Fig. 3. Geometrical construction of the caustic formed by reflections from the rear face of a specimen with an inclined central crack at an angle 45° to the direction of the uniaxial tensile load at infinity from its initial curve of radius $r_{0,r}$ (circles), and of the caustic formed by reflections from the front face of the specimen with its corresponding initial curve of radius $r_{0,f}$ (broad line) for a plexiglas plate with $2c_r/(\nu/E) = 2{\cdot}68$.

Referring the complex function $\Phi(z)$ at the close vicinity of the crack tip by the transformation $\zeta = (z - a)$ we obtain

$$\Phi(z) = -\frac{\sigma(e^{2i\alpha} - 1)}{4} \frac{\zeta + a}{\sqrt{\zeta}\sqrt{\zeta + 2a}}. \tag{32}$$

By developing the term $(\zeta + 2a)^{-1/2}$ into a power series form of $\zeta/2a$ and neglecting the powers of ζ/a we obtain for $\Phi(z)$

$$\Phi(z) = -\frac{\sigma(e^{2i\alpha} - 1)}{4} \sqrt{\frac{a}{2\zeta}}. \tag{33}$$

Relation (33) gives the form of the function $\Phi(z)$ for an oblique central crack of length $2a$ under an angle α with the axis of application of the load, valid only at the close vicinity of the crack tip.

Relation (33), by introducing the opening mode K_I and the sliding mode K_{II} stress intensity factors defined by[7]

$$K_I = \sigma\sqrt{\pi a}, \quad K_{II} = \tau\sqrt{\pi a} \tag{34}$$

where σ is the applied normal stress at infinity normal to the crack axis and τ the corresponding shearing stress, can be written in the form

$$\Phi(z) = \frac{K^*}{2(2\pi\zeta)^{1/2}} \tag{35}$$

where K^* is the complex stress intensity factor given by

$$K^* = (K_I - iK_{II}) \tag{36}$$

Introducing eqn (35) into relations (15) and (16) for the initial curve and the corresponding caustic at the crack tip, we obtain

$$r_0 = |\zeta| = \left[\frac{3CK^*}{2\sqrt{2\pi}}\right]^{2/5} \tag{37}$$

$$W = \zeta \pm \frac{C\bar{K}^*}{\sqrt{2\pi}} \bar{\zeta}^{-3/2} \tag{38}$$

Equation (37) shows that the initial curve for optically isotropic materials is a circle of radius r_0, while the caustic given by both eqns (38) and (37) is a generalized epicycloid. Equation (38), by taking into account relation (37), may be expressed as

$$W = r_0\left(e^{i\theta} \pm \frac{2}{3} \frac{\overline{K^*}}{|K^*|} e^{3i\theta/2}\right) \tag{39}$$

By putting

$$K^* = |K^*| e^{-i\omega}, \quad K_I = |K^*| \cos\omega, \quad K_{II} = |K^*| \sin\omega$$
$$\tan\omega = \frac{K_{II}}{K_I} = \mu \tag{40}$$

relation (39) yields

$$W = r\left(e^{i\theta} \pm \frac{2}{3} e^{(3\theta/2+\omega)i}\right) \tag{41}$$

which, in parametric form, may be written as

$$X = r_0\left[\cos\theta + \frac{2}{3}(1+\mu^2)^{-1/2}\cos\left(\frac{3\theta}{2}\right) - \frac{2}{3}\mu(1+\mu^2)^{-1/2}\sin\left(\frac{3\theta}{2}\right)\right]$$
$$Y = r_0\left[\sin\theta + \frac{2}{3}(1+\mu^2)^{-1/2}\sin\left(\frac{3\theta}{2}\right) + \frac{2}{3}\mu(1+\mu^2)^{-1/2}\cos\left(\frac{3\theta}{2}\right)\right]. \tag{42}$$

The families of generalized epicycloids represented by eqns (42) for various values of $r = r_0$ can be traced if, from every point of the circumference (r, θ) with center the origin of coordinates $O'x'y'$ (Fig. 3), a vector $\mathbf{P'Q'}$ of magnitude $(\frac{2}{3})(1+\mu^2)^{-1/2}r$ is drawn, which makes an angle $3\theta/2$ with the x'-axis. From the end of this vector, another vector $\mathbf{Q'R'}$ is drawn counterclockwise orthogonal to the latter and of magnitude $(\frac{2}{3})(1+\mu^2)^{-1/2}r$. From all curves thus drawn for various r-values, the epicycloid drawn with $r = r_0$ is the principal envelope, which has the property of defining a surface of minimum area.

If we refer the epicycloid to a new coordinate system with the same origin as the latter but angularly displaced by an angle (-2ω), we obtain for the parametric equations of the epicycloid the relations

$$X' = r_0\left[\cos(\theta + 2\omega) \pm \frac{2}{3}\cos 3\left(\frac{\theta}{2} + \omega\right)\right]$$
$$Y' = r_0\left[\sin(\theta + 2\omega) \pm \frac{2}{3}\sin 3\left(\frac{\theta}{2} + \omega\right)\right]. \tag{43}$$

Putting $(\theta + 2\omega) = \varphi$ in relations (43), we obtain

$$X' = r_0\left(\cos\varphi + \frac{2}{3}\cos\frac{3\varphi}{2}\right)$$
$$Y' = r_0\left(\sin\varphi + \frac{2}{3}\sin\frac{3\varphi}{2}\right). \tag{44}$$

From the two last relations it is concluded that the epicycloid is a symmetrical curve with respect to an axis subtending an angle equal to (-2ω) to the crack line. Furthermore, if the crack axis in a plate under simple tension subtends an angle β with the axis of loading, then K_I and K_{II} are given by [7]

$$K_I = \sigma\sqrt{\pi a}\sin^2\beta, \quad K_{II} = \sigma\sqrt{\pi a}\sin\beta\cos\beta \tag{45}$$

so that, from relations (40), we obtain

$$\frac{K_{II}}{K_I} = \cot\beta = \tan\omega.$$

Thus, the angle ω must be equal to the inclination of the axis of the crack with the transverse axis of the plate. Therefore, the axis of symmetry of the caustics is symmetric to the crack-axis with respect to the axis of the load of the plate.

From eqns (44) we obtain for the polar radius ρ of the caustic

$$\rho = (X'^2 + Y'^2)^{1/2} = \left(\frac{13}{9} + \frac{4}{3}\cos\frac{\varphi}{2}\right)^{1/2}. \tag{46}$$

From this relation it can be derived that the polar radius ρ presents an extreme for $\varphi = 0, 2\pi, \ldots$, where it is valid that

$$\rho_{\max} = \frac{5}{3}r_0 \quad \text{and} \quad \rho_{\min} = \frac{r_0}{3}.$$

Furthermore it can be derived that the diameter of the caustic along its axis of symmetry is equal to $D_l = 3r_0$, while the transverse diameter of the caustic is $D_t = 3{\cdot}163\, r_0$.

Figure 3 presents the caustic and its geometrical construction for an oblique crack subtending an angle $\beta = 45°$ to the axis of the applied stress σ at infinity. The external part of the caustic (curve FEDKCBLAG), the geometrical construction of which is shown in this figure, is formed by reflections from the rear face of the plate and corresponds to $C_r = -2z_r dc_r$. This part stops at the reflections from the lips of the crack (points F, G in Fig. 3). The internal part of the caustic is formed from the front face (curve GMLF) of the plate with $C_f = -z_f(\nu/E)d$. While for $C_f = C_r$ the two parts of the caustic have two common points, when $C_f \neq C_r$ a discontinuity between these two parts exists. Figure 3 shows the relative position of the two parts of the caustic formed by reflections for a plexiglas plate containing an internal crack. The ratio of the radii of the corresponding initial curves of the two parts of the reflected caustics is equal to

$$\frac{r_r}{r_f} = 1{\cdot}48.$$

DISCUSSION

Having defined the caustics corresponding to the two extreme cases (the circular hole and the crack), we study now the evolution of caustic from the one to the other extreme case. The corresponding caustics of the two limiting cases are shown in Figs. 2 and 3. While the caustics for the hole are two infinity-shaped curves angularly displaced by 90° (Fig. 2), the caustics for the crack are two cardoid-shaped curves developed separately around the tips of the crack. It is of interest to study the evolution of the shape of caustics from the one to the other limiting case as function of the ellipticity of the ellipse m.

The system of eqns (21) and (22) can only be solved numerically. By putting $z = re^{i\theta}$ into eqn (21) we can define r, using as a parameter the angle θ, which is varying between zero and 360° by steps of 10°. Having traced the initial curve for each case of ellipticity and orientation of the ellipse relatively to the axis of loading we can readily define the corresponding caustic. The numerical solution of eqn (21) yields two roots for z which, when introduced into eqn (22) yield two pairs of values for W. From the system of eqns (21) and (22) defining the caustic it is concluded that this curve depends on the non-dimensional quantity $(C\sigma R^{-2})$, the ellipticity m and the angle α of the major axis of the ellipse with the direction of loading.

Figures 4 and 5 present the initial curves and the corresponding caustics for elliptic holes with ellipticities varying between 0·2 and 0·9 for the case when the major axis of the ellipse is normal to the direction of the tensile load applied at the boundary of the perforated plate. The two solutions for the initial curves are marked as i_1 and i_2 respectively, while the corresponding two pairs of caustics are designated as e_1 and e_2. These figures correspond to a value of the constant $C^* = C\sigma R^{-2} = 12$ which is a mean value for the materials and the characteristic elements of the experimental arrangement used in our experiments.

The diagrams for caustics presented in Figs. 4 and 5 may be classified into two groups. The one group, which results from ellipses with ellipticities m between $m = 0$ and $m = 0{\cdot}3$, forms

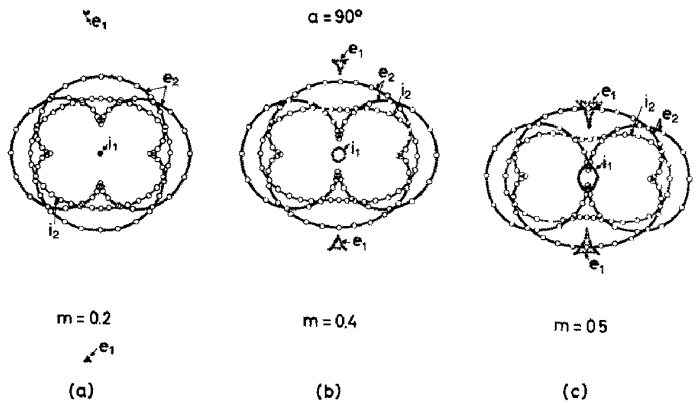

Fig. 4. Initial curves $(i_{1,2})$ and the corresponding caustics $(e_{1,2})$ for elliptic holes with their major axes normal to the direction of the applied load for ellipticities equal to $m = 0{\cdot}2$(a), 0·4(b) and 0·5(c).

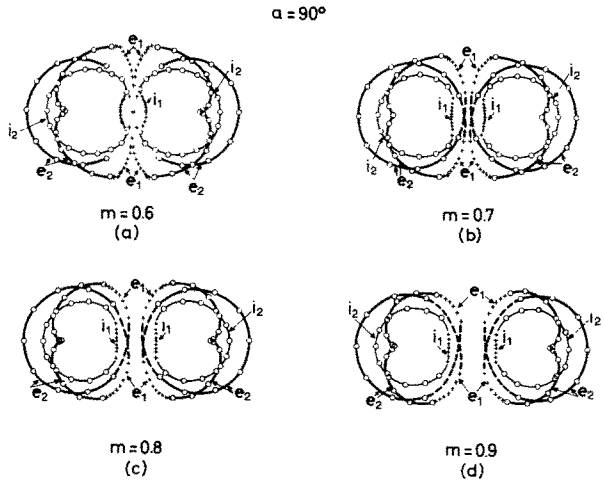

Fig. 5. Initial curves ($i_{1,2}$) and the corresponding caustics ($e_{1,2}$) for elliptic holes with their major axes normal to the direction of the applied load for ellipticities equal to $m = 0{\cdot}6$(a), $0{\cdot}7$(b), $0{\cdot}8$(c) and $0{\cdot}9$(d).

caustics which are continuous and follow the boundary of the elliptic hole. These caustics are similar to the caustics corresponding to circular holes shown in Fig. 2. The other group of caustics, which corresponds to ellipticities larger than $m = 0{\cdot}5$ contains caustics divided into two parts, each of which corresponds to either extremity of the major axis of the ellipse. These caustics resemble more and more, as the ellipticity is increasing, to the caustics obtained from internal cracks (which are considered as ellipses with $m = 1{\cdot}0$).

In this manner the evolution of the caustics formed around perforated plates subjected to axial loading can be followed as the ellipticity is increasing. It is worthwhile noting that the one pair of caustics (e_1) is tending to infinity as the ellipticity is approaching zero. This pair is created from an initial curve, which tends to a point at the center of the hole. As the ellipticity is increasing the i_1-curve is increasing and becomes more and more oblong, while the two pairs of caustics are divided into two parts each, and later on, when m increases above $m = 0{\cdot}6$, the two parts of each pair are combined into one continuous curve at either extremity of the major axis of the ellipse. This type of caustics resembles the caustics formed at the tips of an internal crack (see Fig. 3).

If the major axis of the ellipse is oblique relatively to the axis of loading, the same phenomena are developed with varying ellipticities, but with the corresponding initial curves and caustics distorted.

Figure 6 presents the initial curves and the corresponding caustics for an oblique elliptical hole relatively to the axis of application of the applied load at infinity, under an angle $\alpha = 45°$, for ellipticities equal to $0{\cdot}1$(a), $0{\cdot}4$(b), $0{\cdot}5$(c) and $0{\cdot}8$(d). We observe from this figure that for $m > 0{\cdot}4$ the caustics are separated into two parts as in the case of Fig. 5. Finally, Fig. 7 presents the initial curve and the caustics for an ellipse with its major axis parallel to the axis of the applied load ($\alpha = 0$) for $m = 0{\cdot}3$(a), $0{\cdot}4$(b), $0{\cdot}6$(c) and $0{\cdot}9$(d). The caustics of this figure are separated for

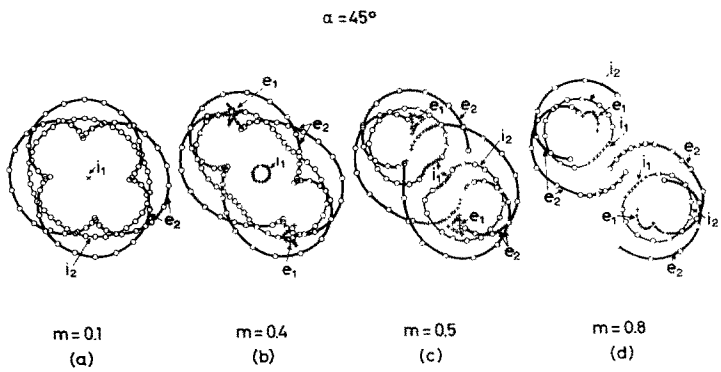

Fig. 6. Initial curves ($i_{1,2}$) and the corresponding caustics ($e_{1,2}$) for elliptic holes with their major axes under an angle equal to $\alpha = 45°$ to the direction of the applied load for ellipticities equal to $m = 0{\cdot}1$(a), $0{\cdot}4$(b), $0{\cdot}5$(c) and $0{\cdot}8$(d).

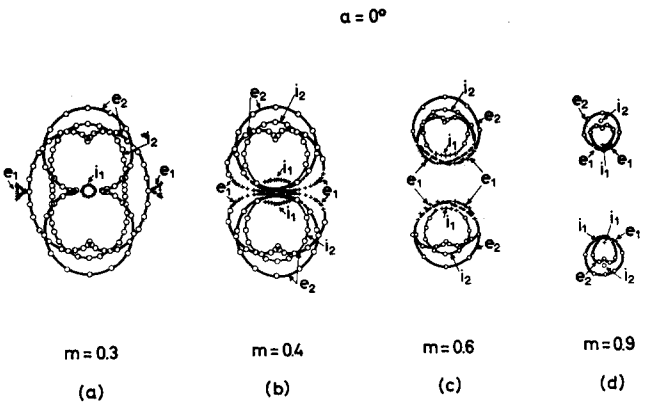

Fig. 7. Initial curves ($i_{1,2}$) and the corresponding caustics ($e_{1,2}$) for elliptic holes with their major axes parallel to the direction of the applied load for ellipticities equal to m = 0·3(a), 0·4(b), 0·6(c) and 0·9(d).

$m > 0{\cdot}3$, while as m increases the caustics become more and more smaller tending to a pair of points for $m = 1$, corresponding to either tip of a crack parallel to the axis of loading. This latter result is in accordance with the theory, since for $m = 1$ the stress function $\Phi(z)$ given by eqn (31) equals zero. These two last figures correspond again to $C^* = C\sigma R^{-2} = 12$ as Figs. 4 and 5.

From Figs. 4–7 it is concluded that the critical value m_{cr} of the ellipticity m for which there is a transition from the one to the other type of caustics depends on the global constant $C^* = C\sigma R^{-2}$ and the angle α between the axis of the ellipse and the direction of the applied load at infinity. This critical value of the ellipticity for which the caustics start to separate can be found by defining the caustics through relations (21) and (22) for various values of the global constant C^* and the angle α. Figure 8 presents the critical value m_{cr} of the ellipticity for C^* varying between 0 and 16 and for the angles $\alpha = 15°, 30°, 45°, 60°, 75°$ and $90°$. We observe from this figure that m_{cr} increases as the constant C^* and the angle α increase.

In order to compare the theoretically obtained results with the experiments a series of tests were undertaken with thin plexiglas plates under simple tension at infinity, each of which contained a central small ellipse with the major axis equal to $2a = 8$ mm, of different ellipticity m,

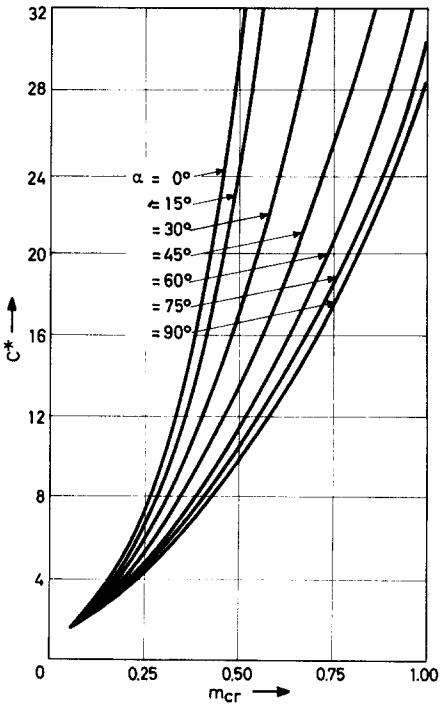

Fig. 8. Variation of the critical value of ellipticity m_{cr} for which the caustics start to separate, vs the global constant C^* varying between 0 and 32 for the following values of the inclination α of the major axis of the ellipse relatively to the direction of the applied load at infinity $\alpha = 0°, 15°, 30°, 45°, 60°, 75°$ and $90°$.

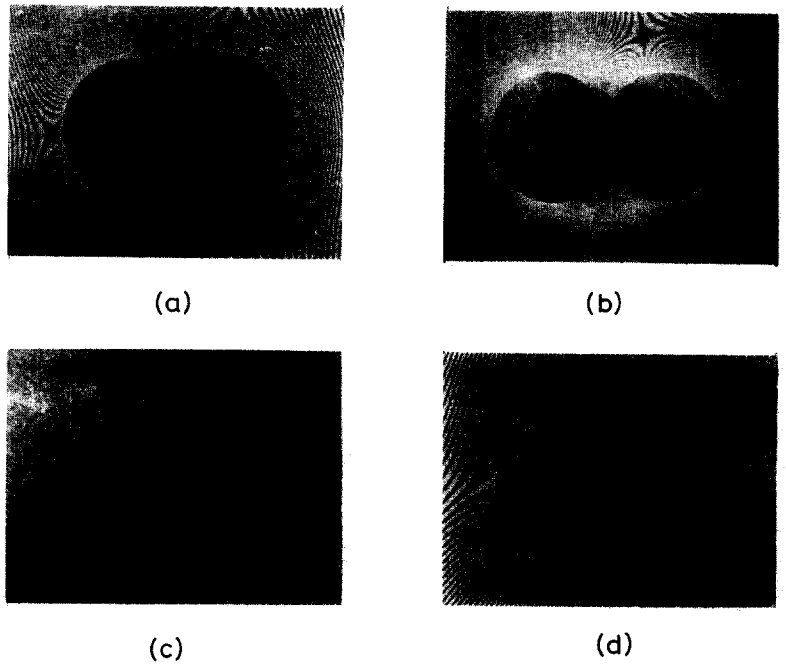

Fig. 9. Experimentally obtained caustics around elliptical holes normal to the direction of the applied load with m 0·132(a) and 0·218(b) and elliptic holes inclined to an angle equal to $\alpha = 45°$ with $m = 0·132$(c) and 0·333(d) respectively.

and different orientation relatively to the axis of the applied load. The width of the plates w was taken equal to $w = 50$ mm and the thickness $d = 2$ mm. The plexiglas plates were conveniently selected with almost flat lateral faces. The plates were interposed in a monochromatic light beam emitted by a He–Ne gas laser. The light beam was widened by a system of lenses, before it impinged on the plate. The reflected beams were received on a ground glass screen placed at a distance $z_r = 181·0$ cm. The magnification ratio λ_i of the optical set-up was $\lambda_i = 6·80$. A progressively increasing tensile load was applied on each specimen, by an Instron tester of capacity of 500 Kp. Each test was terminated with the fracture of the specimen. A photographic camera recorded the interferogram and the caustic formed on the screen at each step of load. Figures 9a and 9b present the caustics around a central elliptical hole with its major axis normal to the direction of loading ($\alpha = 90°$) for ellipticities equal to $m = 0·132$ and $m = 0·218$ respectively. We can observe from these two photographs that as the ellipticity of the hole increases the caustics separate, tending to their complete separation corresponding to the case of crack. It is also pointed out that for the case of Fig. 9a with the hole approaching the circle ($m = 0·132$) the caustic formed from the front faces of the specimen is smaller than that formed from the rear face, the relative position and the dimensions of these two caustics being in accordance with the theoretically obtained forms, shown in Fig. 2. Finally Figs. 9c and 9d show the caustics around an inclined to the direction of application of the load ellipse with an angle equal to $\alpha = 45°$ for $m = 0·132$ and 0·33 respectively. We can observe from these figures that the caustics are distorted as it was predicted by the theory. All caustics of Fig. 9 correspond to a uniaxial tensile load at infinity equal to $P = 200$ Kp. By comparing the shape and size of all these caustics with their corresponding theoretical forms a good agreement can be established between theory and experiment. The discrepancies between the theoretically obtained caustics and those yielded by experiment did not exceed in the main dimensions of caustics five per cent. This agreement allows the use of the caustic as a potential means for accurately analysing the near to the small elliptic hole stress field and evaluating the stress concentration factors around the elliptic perforation.

For this purpose it is possible to drill small elliptic holes conveniently placed and properly oriented all over a biaxial plane stress field. These holes during loading of the plate develop typical caustics, whose size and orientation depend solely on the biaxial stress field, which dominates at the small area where the elliptic hole is drilled, provided that the disturbance of the stress field due to the existence of the hole is negligible.

By assigning two characteristic points on the ellipses and defining their position on the

corresponding caustic during loading, it may be proved that it is possible to evaluate the individual values of the principal stresses at the region of the hole and their orientation.

The same idea for the analysis of particular points in plane-stress fields has already been introduced by the author [3] by drilling small circular holes in the elastic field under evaluation. The thus introduced "circular stress-rosette" yielded directly the principal stress difference and the principal orientation. The "elliptic hole stress-rosette" presents the advantage over the circular stress-rosette that it yields directly the individual values of principal stresses and the principal orientation of the stress field at the small area where the small elliptic hole is drilled. The details of the technique of this method will be presented in a companion paper.

REFERENCES

1. P. S. Theocaris, Local yielding around a crack-tip in plexiglas. *J. Appl. Mech.* **37**, 409 (1970).
2. P. S. Theocaris, Stress singularities due to uniformly distributed loads along straight boundaries. *Int. J. Solids Structures* **9**, 655 (1973).
3. P. S. Theocaris, The reflected shadow method for the study of constrained zones in cracked plates. *Appl. Optics* **10**, 2240 (1971).
4. P. S. Theocaris and E. Gdoutos, An interferometric method for the direct evaluation of principal stresses in plane-stress fields. *J. Physics D* **7**, 472 (1974).
5. M. Born and E. Wolf, *Principles of Optics*, 4th Edn p. 110. Pergamon Press, Oxford (1970).
6. N. I. Muskhelishvili, *Some Basic Problems of the Mathematical Theory of Elasticity*, 2nd Edn. Noordhoff, Amsterdam (1963).
7. P. C. Paris and G. C. Sih, Stress analysis of cracks. Fracture toughness testing and its applications. *A.S.T.M. Sp. Tech. Publ. No.* 381,30 (1965).